APPENDIX A
THE LINEAR APPROXIMATION OF SPHERICAL GAUSSIAN

In the following, we give the linear approximation of the spherical gaussian within a cell.

As the approximation is defined as 1D polynomial functions respective to the dot product, $(\mathbf{v} \cdot \mathbf{p})$, we first project the cell to that 1D domain to compute a interval $[a, b]$ and then approximate the Gaussian by 1-order Legendre polynomials.

Given the four corner vertices of the cell, $\mathbf{c}_0(\varphi_0, \theta_0), \mathbf{c}_1(\varphi_1, \theta_0), \mathbf{c}_2(\varphi_1, \theta_1), \mathbf{c}_3(\varphi_0, \theta_1)$, if the lobe axis does not lie in the cell, the interval is computed as $a = \{\min(\mathbf{c}_i \cdot \mathbf{p}) | i = 0 \text{ to } 3\}$ and $b = \{\max(\mathbf{c}_i \cdot \mathbf{p}) | i = 0 \text{ to } 3\}$. If the lobe axis lies in the cell, then $b = 1$ and a is computed as $a = \{\min(\mathbf{c}_i \cdot \mathbf{p}) | i = 0 \text{ to } 3\}$. Similarly, if the opposite of the lobe axis lies in the cell, then $a = -1$ and $b = \{\max(\mathbf{c}_i \cdot \mathbf{p}) | i = 0 \text{ to } 3\}$.

We need to find optimal coefficients (α, β), so that the polynomial $\alpha + \beta x$ is a optimal approximation of Guassian $G(x) = \mu e^{\lambda(x-1)}$ in the interval $x \in [a, b]$ in the least-square sense. We first map the domain of the problem from $[a, b]$ to $[-1, 1]$ through variable substitution $x = \frac{a+b}{2} + \frac{b-a}{2} t = p + qt$, where $p = \frac{a+b}{2}, q = \frac{b-a}{2}$. Substituting $x(t)$ into the Guassian, we have $G(t) = \mu e^{\lambda(x-1)} = \mu e^{\lambda(p+qt-1)}$, the least-square linear approximation of $G(t)$ is found by projecting it to the normalized Legendre polynomials:

$$P_0(t) = \frac{1}{2}, \quad P_1(t) = \frac{3}{2} t.$$

yields

$$\begin{aligned} r_0 &= (P_0, G(t)) = c \frac{\sinh(\lambda q)}{\lambda q}, \text{ where } c = \mu e^{\lambda(p-1)} \\ r_1 &= (P_1, G(t)) = 3c \frac{\lambda q \cosh(\lambda q) - \sinh(\lambda q)}{\lambda^2 q^2} \end{aligned} \tag{1}$$

Substituting back $t = \frac{x-p}{q}$ into $r_0 + r_1 t$, we get the optimal coefficients of x:

$$\alpha = \left(r_0 - \frac{r_1(a+b)}{b-a} \right), \beta = \left(\frac{2r_1}{b-a} \right) \tag{2}$$

The error of this approximation is measured as

$$e = \int_a^b ||\mu e^{\lambda(x-1)} - (\alpha + \beta x)||_2 dx \tag{3}$$

APPENDIX B
THE ANALYTIC DOUBLE PRODUCT INTEGRALS

In this section, we derive the analytic formation of the double product integral (Eq.(8)). As $\mathbf{p}^*$ and $\mathbf{n}$ are vectors in the space, whose Cartesian coordinate is given by (p_x, p_y, p_z) and (n_x, n_y, n_z), respectively. The dot products $(\mathbf{p}^* \cdot \omega)$ and $(\mathbf{n} \cdot \omega)$ are computed as:

$$\begin{aligned} \mathbf{p}^* \cdot \omega &= p_x \cos\varphi \sin\theta + p_y \sin\varphi \sin\theta + p_z \cos\theta \\ &= u_p \sin(\varphi + \gamma) \sin\theta + v_p \cos\theta \\ \mathbf{n} \cdot \omega &= n_x \cos\varphi \sin\theta + n_y \sin\varphi \sin\theta + n_z \cos\theta \\ &= u_n \sin(\varphi + \tau) \sin\theta + v_n \cos\theta \end{aligned} \tag{4}$$

Substituting these dot products into Eq. (8), we have

$$\begin{aligned} L_o &\approx \int_{\varphi_0}^{\varphi_1} \int_{\theta_0}^{k\varphi+b} (\alpha^* + (\mathbf{p}^* \cdot \omega)) (\mathbf{n} \cdot \omega) \sin\theta \mathrm{d}\theta \mathrm{d}\varphi \\ &= \alpha^* \int_{\varphi_0}^{\varphi_1} \int_{\theta_0}^{k\varphi+b} (\mathbf{n} \cdot \omega) \sin\theta \mathrm{d}\theta \mathrm{d}\varphi \\ &\quad + \int_{\varphi_0}^{\varphi_1} \int_{\theta_0}^{k\varphi+b} (\mathbf{p}^* \cdot \omega) (\mathbf{n} \cdot \omega) \sin\theta \mathrm{d}\theta \mathrm{d}\varphi \\ &= \alpha^* A(\varphi_0, \varphi_1, \theta_0, k, b, \mathbf{n}) + B(\varphi_0, \varphi_1, \theta_0, k, b, \mathbf{n}, \mathbf{p}^*) \end{aligned} \tag{5}$$

where

$$\begin{aligned} &A(\varphi_0, \varphi_1, \theta_0, k, b, \mathbf{n}) \\ &= \int_{\varphi_0}^{\varphi_1} \int_{\theta_0}^{k\varphi+b} (u_n \sin(\varphi + \tau) \sin\theta + v_n \cos\theta) \sin\theta \mathrm{d}\theta \mathrm{d}\varphi \\ &B(\varphi_0, \varphi_1, \theta_0, k, b, \mathbf{n}, \mathbf{p}^*) \\ &= \int_{\varphi_0}^{\varphi_1} \int_{\theta_0}^{k\varphi+b} (u_p \sin(\varphi + \gamma) \sin\theta + v_p \cos\theta) \\ &\quad (u_n \sin(\varphi + \tau) \sin\theta + v_n \cos\theta) \sin\theta \mathrm{d}\theta \mathrm{d}\varphi \end{aligned} \tag{6}$$

Before computing the analytic functions of A and B, we first give some integrals of functions of φ that are used in further derivation.

$$\begin{aligned} C_0(\varphi_0, \varphi_1) &= \int_{\varphi_0}^{\varphi_1} \mathrm{d}\varphi = \varphi_1 - \varphi_0 \\ C_1(\varphi_0, \varphi_1, p) &= \int_{\varphi_0}^{\varphi_1} \sin(\varphi + p) \mathrm{d}\varphi = -\cos(\varphi + p) \Big|_{\varphi_0}^{\varphi_1} \\ C_2(\varphi_0, \varphi_1, s, t) &= \int_{\varphi_0}^{\varphi_1} \cos(s\varphi + t) \mathrm{d}\varphi = \left. \frac{\sin(s\varphi + t)}{s} \right|_{\varphi_0}^{\varphi_1} \\ C_3(\varphi_0, \varphi_1, p) &= \int_{\varphi_0}^{\varphi_1} \varphi \sin(\varphi + p) \mathrm{d}\varphi \\ &= (\sin(\varphi + p) - \varphi \cos(\varphi + p)) \Big|_{\varphi_0}^{\varphi_1} \\ C_4(\varphi_0, \varphi_1, p, s, t) &= \int_{\varphi_0}^{\varphi_1} \sin(\varphi + p) \sin(s\varphi + t) \mathrm{d}\varphi \\ &= \frac{1}{2} \left(\frac{\sin((1-s)\varphi + p - t)}{1-s} - \frac{\sin((1+s)\varphi + p + t)}{1+s} \right) \Bigg|_{\varphi_0}^{\varphi_1} \\ &C_5(\varphi_0, \varphi_1, p, q, s, t) \\ &= \int_{\varphi_0}^{\varphi_1} \sin(\varphi + p) \sin(\varphi + q) \cos(s\varphi + t) \mathrm{d}\varphi \\ &= \left(\frac{\sin(s\varphi + t) \cos(p - q)}{2s} - \frac{\sin((s-2)\varphi + t - p - q)}{4(s-2)} \right. \\ &\quad \left. - \frac{\sin((s+2)\varphi + t + p + q)}{4(s+2)} \right) \Bigg|_{\varphi_0}^{\varphi_1} \end{aligned} \tag{7}$$

where φ_0, φ_1 are integral interval and p, q, s, t are function parameters.

Then, we decompose $A(\varphi_0, \varphi_1, \theta_0, k, b, \mathbf{n})$ and compute it as

$$A(\varphi_0, \varphi_1, \theta_0, k, b, \mathbf{n}) = u_n A_0 + v_n A_1 \tag{8}$$

where,

$$\begin{aligned} A_0 &= \int_{\varphi_0}^{\varphi_1} \int_{\theta_0}^{k\varphi+b} \sin(\varphi+\tau)\sin^2\theta \mathrm{d}\theta\mathrm{d}\varphi \\ &= \int_{\varphi_0}^{\varphi_1} \sin(\varphi+\tau)\left(\frac{2\theta-\sin(2\theta)}{4}\right)\Big|_{\theta_0}^{k\varphi+b}\mathrm{d}\varphi \\ &= \frac{1}{4}\int_{\varphi_0}^{\varphi_1} 2k\varphi\sin(\varphi+\tau) - \sin(2k\varphi+2b)\sin(\varphi+\tau) \\ &+(2b-2\theta_0+\sin(2\theta_0))\sin(\varphi+\tau)\mathrm{d}\varphi \\ &= \frac{1}{4}(2kC_3(\varphi_0,\varphi_1,\tau) - C_4(\varphi_0,\varphi_1,\tau,2k,2b) \\ &+(2b-2\theta_0+\sin(2\theta_0))C_1(\varphi_0,\varphi_1,\tau)) \end{aligned} \tag{9}$$

$$\begin{aligned} A_1 &= \int_{\varphi_0}^{\varphi_1} \int_{\theta_0}^{k\varphi+b} \cos\theta\sin\theta\mathrm{d}\theta\mathrm{d}\varphi \\ &= \int_{\varphi_0}^{\varphi_1} -\frac{1}{2}\cos^2\theta\Big|_{\theta_0}^{k\varphi+b}\mathrm{d}\varphi \\ &= -\frac{1}{2}\int_{\varphi_0}^{\varphi_1}(\cos^2(k\varphi+b)-\cos^2\theta_0)\mathrm{d}\varphi \\ &= -\frac{2(k\varphi+b)+\sin(2k\varphi+2b)}{8k}\Big|_{\varphi_0}^{\varphi_1} + \frac{\cos^2\theta_0}{2}\varphi\Big|_{\varphi_0}^{\varphi_1} \end{aligned} \tag{10}$$

To simplify the notation, we use A_0 and A_1 to represent $A_0(\varphi_0, \varphi_1, \theta_0, k, b, \mathbf{n})$ and $A_1(\varphi_0, \varphi_1, \theta_0, k, b, \mathbf{n})$ respectively. In following, we will use the same notation on B and B_i that B_i is the simplified notation of $B_i(\varphi_0, \varphi_1, \theta_0, k, b, \mathbf{n}, \mathbf{p}^*)$.

After having A, similarly, we decompose $B(\varphi_0, \varphi_1, \theta_0, k, b, \mathbf{n}, \mathbf{p}^*)$ and compute it as

$$\begin{aligned} B(\varphi_0, \varphi_1, \theta_0, k, b, \mathbf{n}, \mathbf{p}^*) &= u_p u_n B_0 + u_p v_n B_1 \\ &+ v_p u_n B_2 + v_p v_n B_3 \end{aligned} \tag{11}$$

$$\begin{aligned} B_0 &= \int_{\varphi_0}^{\varphi_1} \int_{\theta_0}^{k\varphi+b} \sin(\varphi+\gamma)\sin(\varphi+\tau)\sin^3\theta\mathrm{d}\theta\mathrm{d}\varphi \\ &= \int_{\varphi_0}^{\varphi_1} \sin(\varphi+\gamma)\sin(\varphi+\tau)\ \frac{\cos(3\theta)-9\cos\theta}{12}\Big|_{\theta_0}^{k\varphi+b}\mathrm{d}\varphi \\ &= \frac{1}{12}(C_5(\varphi_0,\varphi_1,\gamma,\tau,3k,3b) - 9C_5(\varphi_0,\varphi_1,\gamma,\tau,k,b) \\ &-(\cos(3\theta_0)-9\cos\theta_0)C_4(\varphi_0,\varphi_1,\gamma,1,\tau)) \end{aligned} \tag{12}$$

As B_1 and B_2 have similar forms, we only give the derivation of B_1 and directly give the analytic form of B_2.

$$\begin{aligned} B_1 &= \int_{\varphi_0}^{\varphi_1} \int_{\theta_0}^{k\varphi+b} \sin(\varphi+\gamma)\cos\theta\sin^2\theta\mathrm{d}\theta\mathrm{d}\varphi \\ &= \int_{\varphi_0}^{\varphi_1} \sin(\varphi+\gamma)\ \frac{3\sin\theta-\sin(3\theta)}{12}\Big|_{\theta_0}^{k\varphi+b}\mathrm{d}\varphi \\ &= \frac{1}{12}(3C_4(\varphi_0,\varphi_1,\gamma,k,b) - C_4(\varphi_0,\varphi_1,\gamma,3k,3b) \\ &-(3\sin\theta_0-\sin(3\theta_0))C_1(\varphi_0,\varphi_1,\gamma)) \end{aligned} \tag{13}$$

$$\begin{aligned} B_2 &= \frac{1}{12}(3C_4(\varphi_0,\varphi_1,\tau,k,b) - C_4(\varphi_0,\varphi_1,\tau,3k,3b) \\ &-(3\sin\theta_0-\sin(3\theta_0))C_1(\varphi_0,\varphi_1,\tau)) \end{aligned} \tag{14}$$

$$\begin{aligned} B_3 &= \int_{\varphi_0}^{\varphi_1} \int_{\theta_0}^{k\varphi+b} \cos^2\theta\sin\theta\mathrm{d}\theta\mathrm{d}\varphi \\ &= \int_{\varphi_0}^{\varphi_1} -\frac{\cos(3\theta)+3\cos\theta}{12}\Big|_{\theta_0}^{k\varphi+b}\mathrm{d}\varphi \\ &= -\frac{1}{12}(C_2(\varphi_0,\varphi_1,3k,3b) + 3C_2(\varphi_0,\varphi_1,k,b) \\ &-(\cos(3\theta_0)+3\cos\theta_0)C_0(\varphi_0,\varphi_1)) \end{aligned} \tag{15}$$

APPENDIX C
ILLUSTRATION OF VISIBILITY BOUNDARY EXTRACTION ALGORITHM

To demonstrate the ability of our visibility boundary extraction algorithm, We provide some results of boundary extraction of complex occluders in Fig. 1. As explained in Section 5 and detailed in Algorithm 1 of the paper, we control the quality of visibility extraction by iterative subdivision. The process is controlled by a threshold that takes into account the boundary extraction error. Similar approach was taken by Frisken et al. [18] to approximate shapes by distance fields. While the proof of conservativeness can be difficult, in practice we find the approach works well even for complicated visibility functions. As can be seen from these examples, by controlling the error threshold e_r, we are able to increase the accuracy of boundary extraction and catch disconnected visibility regions and some wiggles Fig. 1(b).

APPENDIX D
QUALITY AND PERFORMANCE TRADE-OFF

In our method, we take an adaptive subdivision scheme to extract visibility boundaries. In such a way, it allows users to make tradeoff between shadow quality and performance. In Fig. 2, we show results with different shadow quality and performance. It can be observed that by tweaking the error threshold more cells are generated and higher quality of soft shadows can be obtained, and performance declines accordingly.

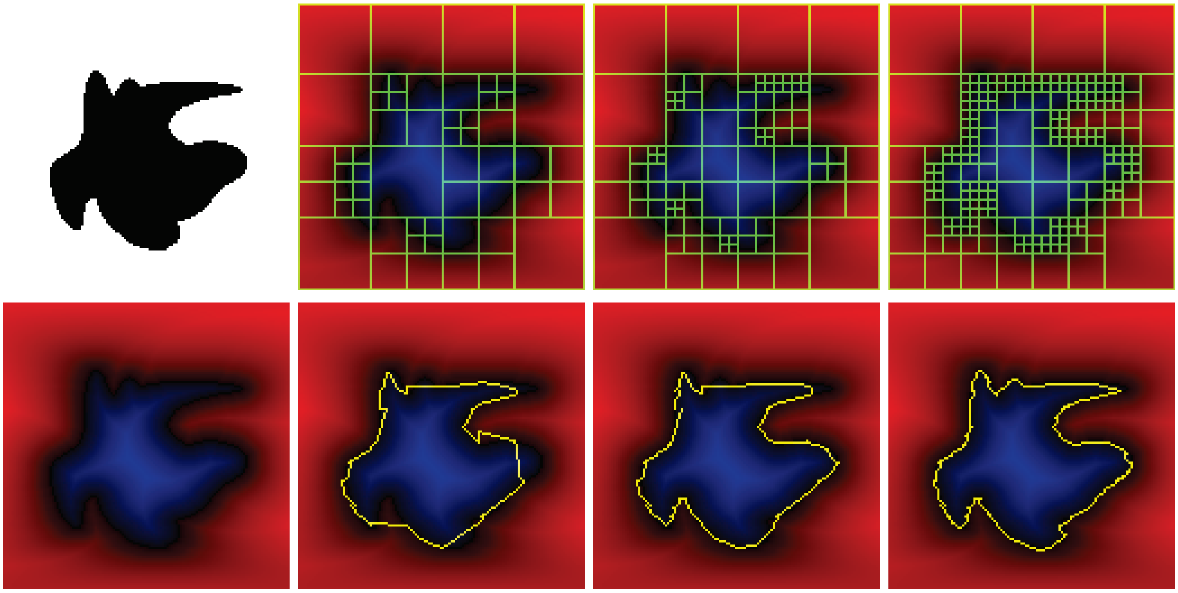

(a) Visible region and the SSDF (b) $e_r = 0.2$ (c) $e_r = 0.04$ (d) $e_r = 0.008$

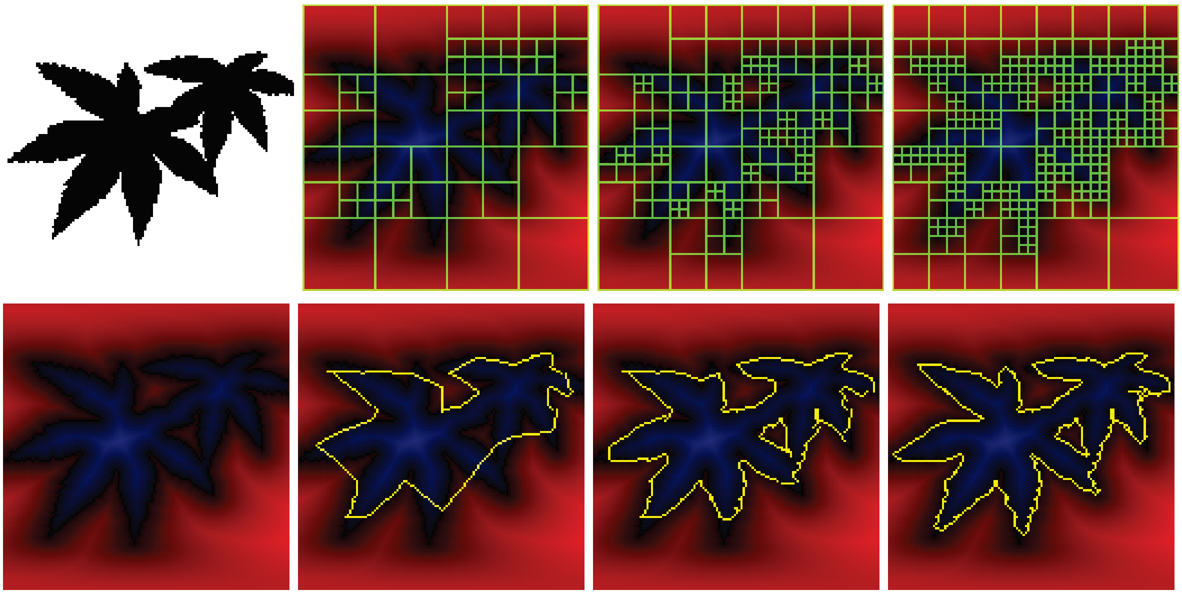

(e) Visible region and the SSDF (f) $e_r = 0.2$ (g) $e_r = 0.04$ (h) $e_r = 0.008$

Fig. 1. Extracting the boundary of complex occluders. (a) and (b) are two visible regions with different complex boundaries. Cells and extracted boundaries under different threshold e_r are shown.

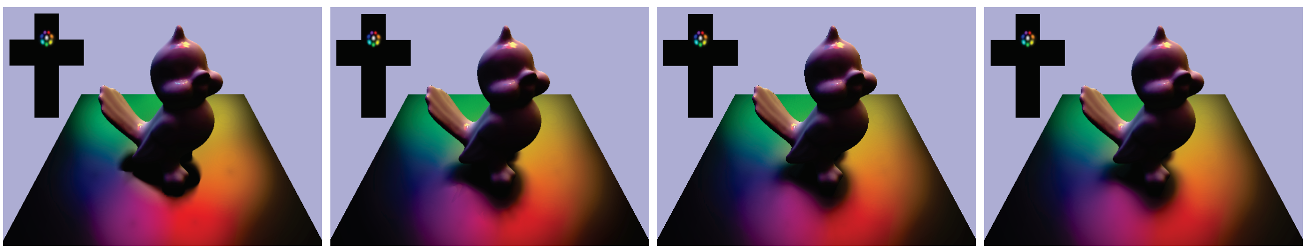

(a) $n_{avg} = 1$, FPS 85.0 (b) $n_{avg} = 3.3$, FPS 51.5 (c) $n_{avg} = 8.5$, FPS 35.1 (d) $n_{avg} = 13.8$, FPS 22.7

Fig. 2. Demonstration of the quality and performance trade-off, n_{avg} is the average number of cells generated per pixel.